Electrochemical Behavior of Serratia marcescens ACE2 on Carbon Steel API 5LX60 in Organic/Aqueous Phase

ARTICLE *in* INDUSTRIAL & ENGINEERING CHEMISTRY RESEARCH · SEPTEMBER 2008

Impact Factor: 2.59 · DOI: 10.1021/ie8005935

3 AUTHORS, INCLUDING:

Aruliah Rajasekar
TVU
27 PUBLICATIONS **354** CITATIONS
SEE PROFILE

Yen-Peng Ting
National University of Singapore
132 PUBLICATIONS **4,312** CITATIONS
SEE PROFILE

MATERIALS AND INTERFACES

Electrochemical Behavior of *Serratia marcescens* ACE2 on Carbon Steel API 5L-X60 in Organic/Aqueous Phase

Aruliah Rajasekar,*,† Sundaram Maruthamuthu,‡,§ and Yen-Peng Ting†

Department of Chemical and Biomolecular Engineering, National University of Singapore, 4 Engineering Drive 4, Singapore 117576, and Garrett Block, Microbial Corrosion, Central Electrochemical Research Institute, Karaikudi, 630 006, India

The present study reports on the role of the bacterium *Serratia marcescens* ACE2 in the corrosion behavior of carbon steel API 5L-X60 in diesel−water systems. The effect of commercial corrosion inhibitor (CI) on the growth of strain ACE2 and its corrosion inhibition efficiency was investigated. The corrosion rate was evaluated using electrochemical impedance spectroscopy (EIS) and polarization techniques in the diesel−water interface systems. The amine and carboxylic acid based inhibitor gave better efficiency in the absence of strain ACE2 by suppression of both anodic and cathodic reactions. In the presence of the strain ACE2, the inhibitor suppressed the cathodic reaction more significantly than the anodic reaction. The electrochemical behavior of steel API 5L-X60 was correlated with the role of the adsorbed amine based compound and degraded product on the metal surface. The surface morphology of the coupons in the presence/absence of the inhibitor with ACE2 was observed by using atomic force microscopy (AFM) and revealed pitting corrosion. This basic study is useful for the development of new approaches for the detection, monitoring, and control of microbial corrosion in a petroleum product pipeline.

1. Introduction

Corrosion is a major cause of pipeline failure and is a significant component affecting the operation and maintenance costs of gas industry pipelines.[1–5] The estimated pipeline corrosion loss to the gas industry in 1996 was about $840 million/year,[2] while the estimated annual cost of all forms of corrosion to the oil and gas industries in 2001 was $13.4 billion, of which microbially influenced corrosion accounted for about $2 billion.[5] Studies on corrosion of metals in organic−aqueous phase have attracted considerable interest in recent years due to their common occurrence in pipelines transporting petroleum products.[6–10] It has been reported that corrosion caused by aqueous organic solvents can be effectively controlled by the use of corrosion inhibitors.[11–14] Most of the efficient inhibitors used in industry are organic compounds, which mainly contain nitrogen, sulfur atoms, and multiple bonds in the molecules through which they are adsorbed on the metal surface. Nitrogen-containing heterocyclic compounds are considered to be effective corrosion inhibitors. Organic film-forming inhibitors used in the oil and gas industry are generally of the cationic/anionic type and include imidazolines, primary amines, diamines, amino-amines, oxyalkylated amines, fatty acids, dimer, trimer acids, naphthaneic acid, phosphate esters, and dodecylbenzenesulfonic acids. Their mode of action is the formation of a persistent monolayer film adsorbed at the metal/solution interface.[15–17] The alteration of molecules of corrosion inhibitor at oil−water interface is due to microbial degradation, which can affect their specific performance on corrosion inhibition.[18–20]

The inactivation or killing of the bacteria at the interface would effectively inhibit the production of the emulsion[8] and degradation of petroleum products including diesel. Therefore, the identification of inhibitor/biocides that could act at the interface is needed in pipelines transporting petroleum. Hence, bacterial activities on diesel and the corrosion of materials in water have been controlled by the addition of inhibitors which are water dispersible and diesel soluble. In the present study, a commercially available water dispersible (sparingly soluble) inhibitor was selected and the role of *Serratia marcescens* ACE2 on the electrochemical behavior of API 5L-X60 in the presence/absence of corrosion inhibitor was investigated.

2. Experimental Materials and Methods

2.1. Microorganism. *S. marcescens* ACE2 was isolated from a corrosion product at the diesel-transporting pipelines in a northwestern region of India and identified as described earlier.[21] The culture was recharacterized based on the following analyses: morphology, Gram staining, spore staining, motility, oxidase, catalase, oxidative fermentation, gas production, ammonia formation, nitrate and nitrite reduction, indole production test, methyl red and Voges-Proskauer tests, citrate and mannitol utilization test, hydrolysis of casein, gelatin, starch, urea, and lipid.

2.2. Composition of Corrosion Inhibitor (CI). A commercially available corrosion inhibitor (Finocor, India) used in petroleum-transporting pipeline was evaluated to determine its corrosion inhibition efficiency. The inhibitor is an amine-based carboxylic acid compound, and its composition was examined using a Thermo Finnigan gas chromatograph/mass spectrometer equipped with an RTX-5 capillary column 30 m long × 0.25 mm internal diameter and flame ionization detector (FID) and high-purity nitrogen as carrier gas. The oven was programmed between 80 and 250 °C at a heating rate of 10 °C/min. The gas

* To whom correspondence should be addressed. Tel.: + (65) 65162075. E-mail: rajasekar@nus.edu.sg or rajasekargood@gmail.com.
† National University of Singapore.
‡ Central Electrochemical Research Institute.
§ Present address: Electrical Power Research Laboratory, Korea Electrotechnology Research Institute, Chang Won, 641-600, South Korea.

10.1021/ie8005935 CCC: $40.75
Published on Web 08/01/2008

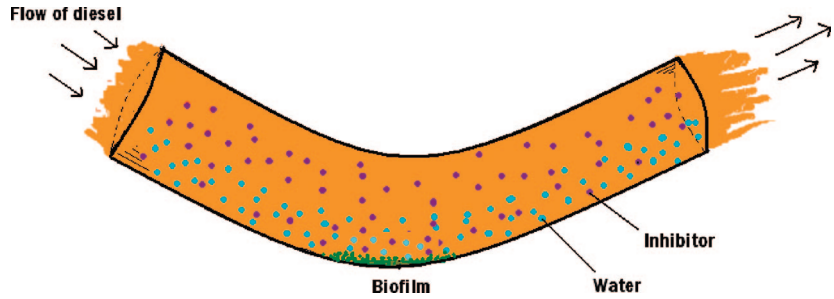

Figure 1. Schematic diagram showing water stagnation point in the internal of a fluid-transporting pipeline.

chromatography (GC) retention data of the inhibitor corresponding to structural assignation was done after an NIST (National Institute of Standards and Technology) library search with a database and by mass spectra interpretation.

2.3. Electrochemical Studies. A carbon steel electrode (API 5L-X60) was constructed by embedding square specimens in epoxy resin. A coupon of 1 cm^2 exposed area of API 5L-X60 as the working electrode, a standard calomel electrode (SCE), and a platinum wire as counter electrode were employed for electrochemical studies.[22] The electrodes were polished using a 600 grit abrasive grade paper, washed in distilled water, surface sterilized by immersion in a 70% ethanol solution for 1 min, and finally dried in warm air.

Electrochemical experiments were performed (using duplicate coupons) at 28 °C. A mixture of diesel and water (containing 120 ppm chloride ion) in the ratio 2:1 was prepared[18] for electrochemical studies. System 1 consisted of 75 mL of 1% BH broth (magnesium sulfate, 0.20 g/L; calcium chloride, 0.02 g/L; monopotassium phosphate 1 g/L; dipotassium phosphate, 1 g/L; ammonium nitrate, 1 g/L; ferric chloride, 0.05 g/L; 120 ppm chloride; pH 7) and 150 mL of diesel. System 2 consisted of system 1 inoculated with 2 mL of inoculum ACE2 at about 10^6 CFU/mL. System 3 consisted of system 1 in the presence of 10 ppm of inhibitor. Finally, system 4 consisted of system 3 in the presence of 2 mL of ACE2 at about 10^6 CFU/mL. The inoculum contained 10^6 CFU/mL for both systems 2 and 4. The colony forming units (CFU) per milliliter was determined using the standard pour plate method. All mixtures were stirred vigorously using magnetic stirring beads for 120 h to simulate field conditions. After 10 days, the coupons were removed and impedance and polarization studies were conducted using the same coupons, with care taken to avoid the disturbance of the oxide film in the presence of bacterium for the polarization study.

Tafel polarization curves were obtained by scanning from the open-circuit potential or corrosion potential (E_{corr}) toward 200 mV anodically and cathodically by employing separate coupons. The scan rate was 120 mV/min. Polarization measurements were carried out potentiodynamically using potentiostat Model PGP201, with volta master-1 software. An EG&G electrochemical impedance analyzer (Model M6310 with software M398) was used for ac impedance measurements between 10 mHz and 100 kHz, with a 5 mV perturbation signal at the corrosion potential.

2.3.1. Atomic Force Microscopy. The extent of corrosion damage caused by ACE2 in the presence/absence of the inhibitor (in systems 3 and 4) was characterized using atomic force microscopy (AFM) analysis. The API 5L-X60 specimens of size $10 \times 10 \times 2.5$ mm were abraded with emery paper (grade 320-500-800-1200) to give a homogeneous surface, and were finally polished to a mirror-finish surface using 0.3 μm alumina powder. The polished coupons were first rinsed with deionized water thrice, followed by degreasing with acetone, then sterilized in 70% ethanol for 4 h, and dried aseptically in air. After the immersion period (in system 4), the specimen was removed and ultrasonic treatment was carried out to remove the biofilm on the metal surface.[23] Pico scan 2100 model (Molecular Imaging, USA) using gold-coated silicon nitride (Si_3N_4) cantilevers (force constant 3 N/m) of 30 nm tip area operated in a contact mode was used to capture the images of the pits on the coupon surface.

2.3.2. Fourier Transform Infrared Spectroscopy (FTIR) Analysis. To verify the adsorption of the corrosion inhibitor and biodegradation on the metal surface, the film formed on the metal surface after 10 days was carefully removed and dried, and mixed thoroughly with 2% potassium bromide (KBr). The mixture was ground into fine powder and compressed into disks using a hydraulic press at 100 kg/cm^2. The pellets were subjected to FTIR analysis (Perkin-Elmer, Nicolet Nexus −470) to determine the protective film formed on the surface of the metal coupons. The nature of the biodegradation was characterized by FTIR analysis. In addition, the adsorption of inhibitor components on the metal surface after 2 h immersion in inhibitor solution at the initial period was characterized by FTIR.

3. Results and Discussion

It has been reported that the growth of prokaryotic and eukaryotic microorganisms on hydrocarbons is often associated with the production of surface-active compounds.[24–26] In general, the degradation of hydrocarbon is accompanied by emulsification, resulting in a more significant oil−water interface.[27] A number of surfactants have been isolated from microbial cultures following the growth of bacteria and fungi on a variety of aliphatic hydrocarbons. These emulsifiers, which are generally extracellular, may be relatively simple glycolipids or complex high-molecular-weight substances, often of uncertain structure.[28–30] Their production allows the uptake and utilization of hydrocarbons and this, in turn, leads to the growth of microbial cells, which has important implications for the oil industry.[8,31] For this reason, the effective inhibition of microbially induced corrosion requires the control of bacterial proliferation at the interface of organic and aqueous phases and the metal surface. Water stagnation in petroleum product pipelines and storage tanks is commonly encountered in the petroleum industry. Microorganisms at the diesel/water interface on materials enhance metal losses and sludge formation by microbial corrosion.[21] Water stagnation and the possibility of abundance of bacteria in the organic−aqueous phase are schematically presented in Figure 1. Hence, the present study is particularly relevant to the petroleum industry, since many suppliers are recommending sparingly soluble inhibitors in water for petroleum-transporting pipelines.

Figure 2 shows polarization curves for API 5L-X60 steel in the various systems. The corrosion currents for system 1 and

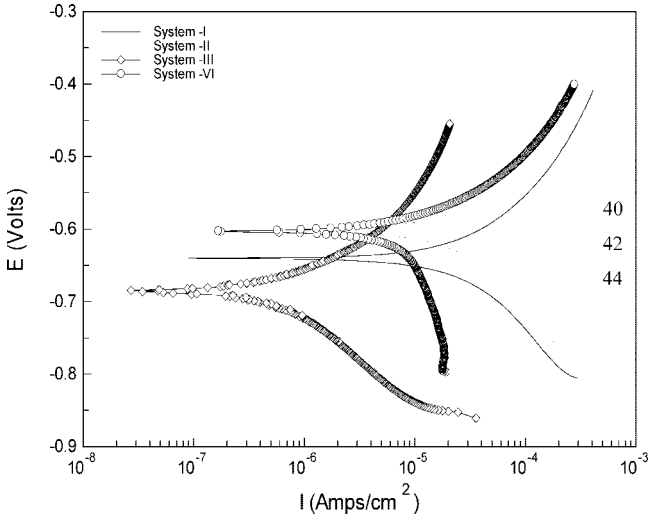

Figure 2. Polarization curves for API 5L-X60 in diesel−water system, in the presence/absence of ACE2 for different systems: system I, 500 mL of diesel + 2% water; system II, 500 mL of diesel + 2% water + ACE2; system III, 500 mL of diesel + 2% water + 10 ppm corrosion inhibitor; system IV, 500 mL of diesel + 2% water + ACE2 + 10 ppm corrosion inhibitor.

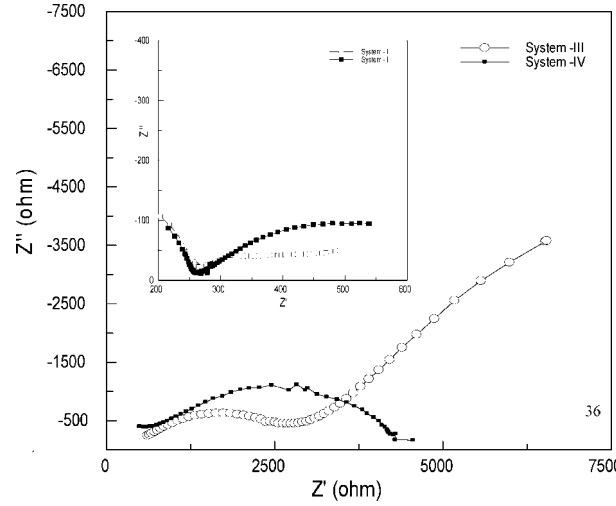

Figure 3. Impedance curves for API 5L-X60 in diesel−water system, in the presence/absence of ACE2 for different systems: system I, 500 mL of diesel + 2% water; system II, 500 mL of diesel + 2% water + ACE2; system III, 500 mL of diesel + 2% water + 10 ppm corrosion inhibitor; system IV, 500 mL of diesel + 2% water + ACE2 + 10 ppm corrosion inhibitor.

that inoculated with ACE2 (system 2) were 2.95×10^{-5} and 2.93×10^{-5} A/cm^2 respectively (Table 1). The corrosion potentials for system 1 were −639 and −601 mV for the control and system 2, respectively. This indicates that the potential of carbon steel was shifted by ACE2 toward the anodic side. In the presence of the inhibitor in the organic−aqueous phase (system 3), the open-circuit corrosion potential (E_{corr}) was −685 mV and the corrosion current density (I_{corr}) was 8.07×10^{-7} A/cm^2. In system 4 (ACE2 inoculated with inhibitor in organic−aqueous interface) the E_{corr} was −603 mV and the corrosion current was 1.32×10^{-5} A/cm^2. These results indicate that the inhibitor works better in the absence of strain ACE2. Though the corrosion current was more or less same in both systems 1 and 2, pitting corrosion was noted in the presence of strain ACE2. This is due to the heterogeneity of bacterial corrosion. Even though the inhibitor was added with bacteria in system 4, the corrosion current was not reduced (system 4, 1.32×10^{-5} A/cm^2) when compared to systems 1 and 2. This is due to the biodegradation of inhibitor. The reduction in anodic current can be noted in systems 2 and 3 when compared to system 1. In system 3, a significant reduction in anodic current occurred. It can be explained that the bacterial adsorption reduces the anodic current in system 2, whereas in system 4 the bacterium ACE2 also degrades the organic components and reduces the anodic current. It can be explained that the role of bacterium ACE2 on degradation may influence the anodic current in systems 2 and 4. The bacterium ACE2 has been described in earlier studies,[21] and has been shown to be capable of degrading the corrosion inhibitor as a sole carbon source. The behavior of the anodic curve in system 4 indicates that the water−oil soluble anionic components present in inhibitor control the anodic reaction. Besides, the reduction in cathodic current was noted in systems 3 and 4, indicating that sparingly water soluble components (nitrogen-based components) control the cathodic reaction.

Values of solution resistance (R_s) and the charge transfer resistance (R_{ct}) were derived from impedance measurements and are presented in Table 1 and Figure 3. The R_s values for all the systems fall in the range of 200−436 Ω·cm^2. In systems 1 and 2, the R_{ct} values were 434 and 602 Ω·cm^2, respectively. The addition of the inhibitor increased the resistance to 3.31 kΩ·cm^2. Further, the resistance increased in the presence of ACE2 along with the inhibitor (4.5 kΩ·cm^2). The increase in R_{ct} (4.5 kΩ·cm^2) may be due to the adsorption of the inhibitor and any bacterially degraded product. Improvement of resistance in inhibitor system 3 is due to the adsorption of cation on metal surface, which supports the polarization studies.

In the presence of the inhibitor, the impedance curve shows two capacitive loops. The first capacitive loop is small when compared to the second. The first capacitive loop is well-defined with a high-frequency range. The high-frequency part represents the formation of the intact part of the adsorbed film.[32] In system 4 (presence of ACE2 with inhibitor), a semicircle can be noticed which indicates the activation control (anodic reaction). It reveals that the degraded product of inhibitor adsorbs on the metal surface and influences the electrochemical behavior of the metal. Even though the degraded anionic product of inhibitor enhances

Table 1. Polarization and Impedance Parameters for API 5L-X60 in the Presence/Absence of Inhibitor

		polarization data				impedance data		
system no.	system	E_{corr} (mV)	b_a (mV/decade)	b_c (mV/decade)	I_{corr} (A/cm^2)	R_s (ohm)	R_{ct} (Ω·cm^2)	C_{dl} (Faraday/cm^2)
1	75 mL of 1% BH broth (containing 120 ppm chloride) and 150 mL of diesel	−639	159	166	2.95×10^{-5}	200	434	8.15×10^{-5}
2	75 mL of 1% BH broth (containing 120 ppm chloride) and 150 mL of diesel + ACE2	−601	188	168	2.93×10^{-5}	256	602	2.42×10^{-3}
3	75 mL of 1% BH broth (containing 120 ppm chloride) and 150 mL of diesel + corrosion inhibitor	−685	134	127	8.07×10^{-7}	292	3.31	8.44×10^{-8}
4	75 mL of 1% BH broth (containing 120 ppm chloride) and 150 mL of diesel + ACE2 + corrosion inhibitor	−603	128	431	1.32×10^{-5}	436	4.5	2.96×10^{-7}

Table 2. Gas Chromatography−Mass Spectral Data of Corrosion Inhibitor

retention time (min)	compounds
0.90	1-hexadecanol
1.00	3-nonen-2 one
1.07	1-octadecyne
1.10	cyclohexane, 1-methyl-2-propyl
1.24	2-propenic acid octyl ether
1.35	benzene, 1,2,3,5-tetramethyl
1.72	tetradecane, 1-chloro
1.55	benzene, 1,2-diethyl
11.22	*n*-hexadecanoic acid
13.16	oleic acid
13.35	pyridine, 2-tridecyl
14.30	pyridine, 2-tridecyl
15.14	pyridine, 2-tridecyl
15.94	phenol, 2,6-di(*tert*-butyl)-4-(cyclohexanylidene)amino

Table 3. Solubility Data for the Corrosion Inhibitor Components[47–50]

composition	molecular mass	chemical formula	solubility in water
oleic acid	282.5	$C_{18}H_{34}O_2$	insoluble
aminophenol	109.11	C_6H_7NO	0.60%
diethylbenzene	134.22	$C_{10}H_{14}$	0.0017%
hexadecanoic acid	256.42	$C_{16}H_{32}O_2$	insoluble
pyridine	79.10	C_5H_5N	unlimited solubility

the resistance, the anodic current was more or less same as the control (system 1) in the polarization curve. Hence, the selections of good nonbiodegradable anodic components in a good inhibitor or a good biocide are important criteria for petroleum product pipelines.[33,34] In systems 1 and 2 the first capacitive loop is relatively small when compared to the second. The loop in low frequency is not clearly defined, whereas the low-frequency data points are associated with the Faradaic processes occurring on the bare metal through defects and pores in the adsorbed diesel components on the metal surface. The double layer capacitance (C_{dl}) values were 8.15×10^{-5}, 2.42×10^{-3}, 8.44×10^{-8}, and 2.96×10^{-7} F/cm^2 in systems 1, 2, 3, and 4, respectively. The capacitance of system 1 is due to the corrosion of API 5L-X60 (8.15×10^{-5}). The capacitance was highest in system 2 (with strain ACE2), which is due to the heterogeneity and negative charge of the biofilm on the metal surface.

The capacitance was lower in the presence of the inhibitor (with and without the bacterium ACE2). This indicates that the inhibitor adsorbs and reduces the charges present on the metal surface. The capacitance value of system 4 is higher compared to that of system 3. The enhancement of the capacitance in system 4 may be due to the adsorption of degraded product on the metal surface.

From the GC retention data of the corrosion inhibitor, the structural assignment after the NIST library search with a database and by mass spectral interpretation is presented in Table 2, and the solubility data for the inhibitor components are presented in Table 3. It was observed that the corrosion inhibitor consists of aliphatic hydrocarbons including cyclohexane, octadecyne, *n*-hexadecanoic acid, propenic acid octyl ether, tetradecane, and aromatic carbons including benzene 1,2-diethyl, pyridine, and phenol. The major component is oleic acid. The inhibitor is an amine-based carboxylic acid compound. The solubility data also indicate the nitrogen-based pyridine components dissolve in water and influence the cathodic behavior of API 5L-X60 (Table 2).

The FTIR spectrum of the pure corrosion inhibitor is shown in Figure 4A. The N−H stretching bands in the range of

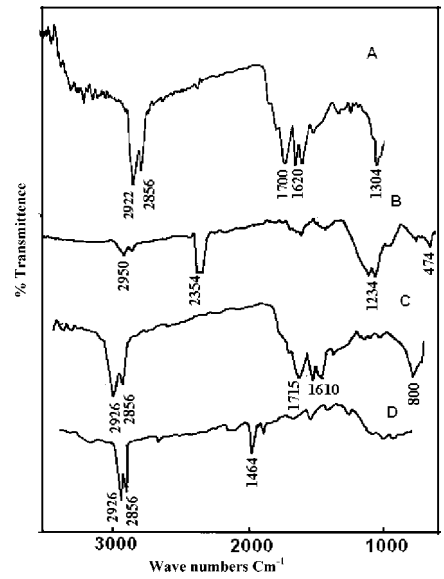

Figure 4. Surface film on the metal surface in the presence of the corrosion inhibitor with ACE2. (A) Pure corrosion inhibitor. (B) Corrosion inhibitor: 2 h immersion period. (C) Corrosion inhibitor: system 3. (D) Corrosion inhibitor with ACE2: system 4.

3250−3400 cm^{-1} and 2662 cm^{-1} are due to the presence of amine group. The aromatic C−H stretching band was observed at 3050 cm^{-1}. The methyl (CH_3) and methylene (CH_2) aliphatic saturated C−H stretching bands were observed at 2922 and 2856 cm^{-1}, respectively. The N−H stretching band can be noticed at 2662 cm^1. The aromatic overtone band or olefinic (=C−H) is observed in the range 1900−1800 cm^{-1}. The C=O stretching band observed at 1700 cm^{-1} is due to the presence of carboxylic acid group. The peaks at 1376 and 1620 cm^{-1} show the presence of carboxylate anion, which confirms the presence of carboylic acid component in the inhibitor. The peak at 1554 cm^{-1} is due to aromatic C=C stretching band, and the peak at 1456 cm^{-1} is due to aromatic C−C stretching band. The C−N asymmetric stretching was observed at 1397 cm^{-1}, and C−N symmetric stretching was observed at 1304 cm^{-1}.

After 2 h immersion of the corrosion inhibitor, the following components were observed (in Figure 4B). The wavenumber 1234 cm^{-1}, indicating the presence of NH group, shows that, within 2 h, pyridine was adsorbed on the metal surface. Peaks at 3250−3400 cm^{-1} (NH), 2914−2840 cm^{-1} (−N−H), 2354 cm^{-1} (−NH−), 1601 cm^{-1} (COO^-), 1416 cm^{-1} (−C=C− stretch for aromatic compounds), 1097 and 1051 cm^{-1} (−C−O− for primary alcohol), 751 and 652 cm^{-1} (disubstituted benzene ring), 544 and 503 cm^{-1} (alcohol −OH out-of-plane bending), and 474 and 415 cm^{-1} (chloride) were detected on the metal surface.

The FTIR spectrum for the inhibitor added in system 3 (after the 10th day) after electrochemical study is shown in Figure 4C. All the peaks observed on the metal surface were similar to that on the metals after 2 h immersion of the inhibitor. The wavenumber 1234 cm^{-1}, however, was not detected. This indicates that pyridine dissolved in water, with minimal adsorption on the metal surface. Peaks at 3300−3400 cm^{-1} indicate the presence of N−H stretching bands. A peak at 2950 cm^{-1} indicates −C−H stretching in the aliphatic components. A peak near 3000 cm^{-1} indicates the presence of =C−H stretching in aromatic components. Peaks at 1370 and 1610 cm^{-1} indicate the presence of carboxylate anion. A peak at 1670 cm^{-1} indicates the −C=C stretch for aliphatic compound, and a peak at 1585 cm^{-1} indicates −C=C stretch for aromatic compound.

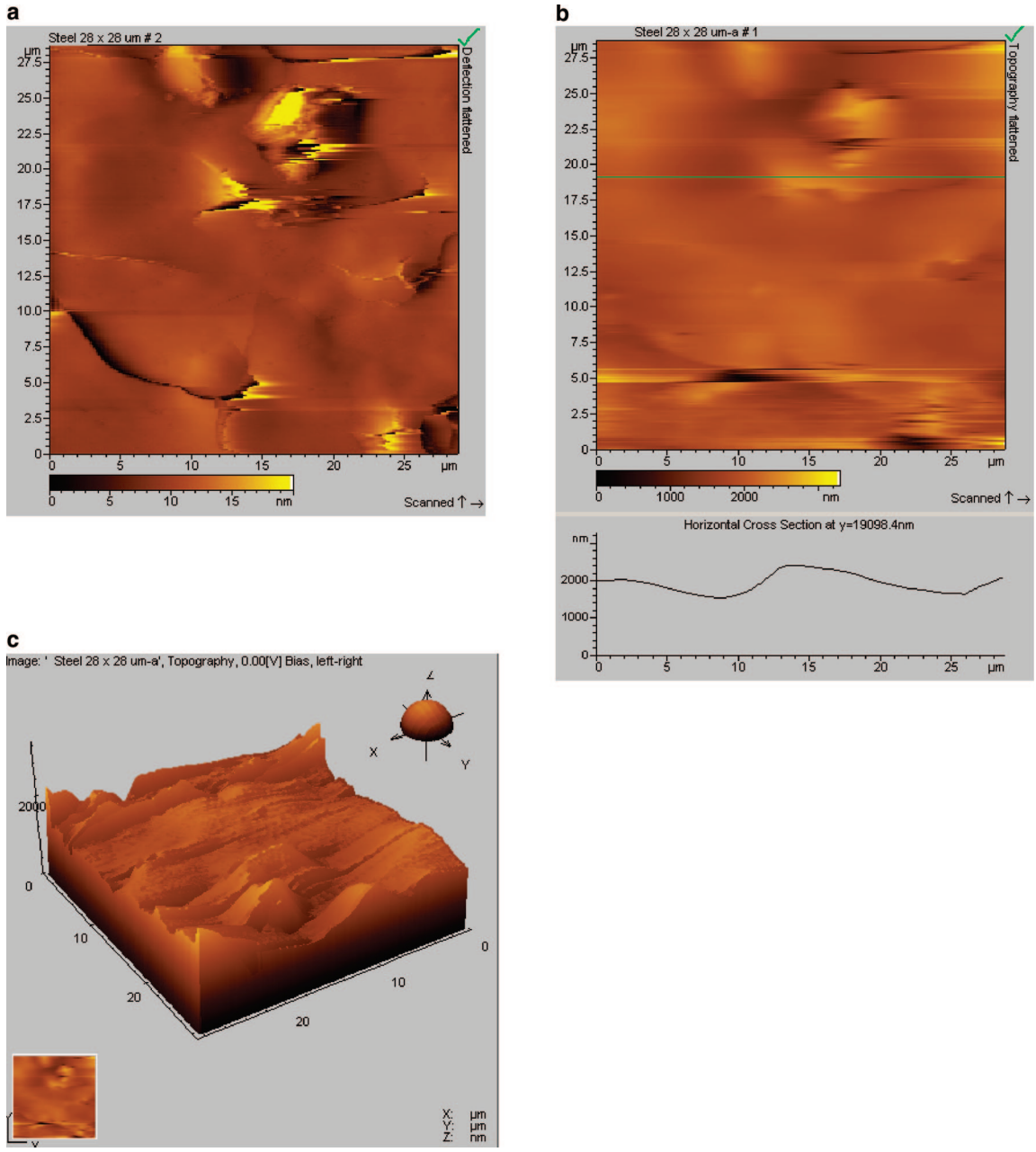

Figure 5. AFM images of API 5L-X60 carbon steel surface exposed to inhibitor system 3. (a) Two-dimensional topographic images of the corroded coupon surface (28 × 28 μm). (b) Cross-sectional analysis determining the surface morphology. (c) Three-dimensional topographic images of the corroded coupon surface steel.

Peaks at 1306 and 1280 cm^{-1} indicate the presence of −C−N stretch for primary aromatic amine, and a peak at 1050 cm^{-1} indicates the presence of −C−O stretch for primary alcohol. The wavenumber 1715 cm^{-1} indicates the presence of an aldehyde group. The aromatic para-disubstituted compounds were observed at 800−850 cm^{-1}. This indicates that the adsorbed corrosion inhibitor consists of amine-based and carboxylic acid (oleic acid) compounds.[35] The major components of −NH− did not adsorb on the metal surface. Although N−H is water soluble, the adsorption is poor. Electrochemical study, however, shows that the water-soluble components N−H suppress the cathodic reaction. The solubility of NH in water suppresses the corrosivity of water along with suppression of cathodic reaction of API 5L-X60.

In the presence of the inhibitor inoculated with ACE2 (Figure 4D), the majority of the peaks at 1554 (C═C), 1456 (−C−C−), 1397 (C−N), 1304 (C−N), and 968 and 722 cm^{-1} (disubstituted benzene) are absent from system 4 on the metal surface. It can be explained that ACE2 utilized the carboxylate anions and cations like NH.[18,19,21] Hence, the corrosion current was more or less same as that for system 1. The inhibitor adsorbed on steel acts as a cathodic inhibitor by retarding the transfer of hydrogen and chloride from the bulk solution to the mild steel/solution interface. Because amine inhibitors function as adsorbates, their inhibition performance primarily relies on the adsorption bond between the atoms in the metal and inhibitor molecules.[36] Sheng et al.[37] reported that the nitrogen atoms in the 2-methylbenzimidazole molecule had an affinity toward mild steel and anchors on the metal surface via the amine bond. Nitrogen-containing organic heterocyclic compounds were considered to be excellent chelate-forming substances with several transition metals.[38–41] This indicates that the efficiency of corrosion inhibitor has been decreased by bacterial degradation.[17]

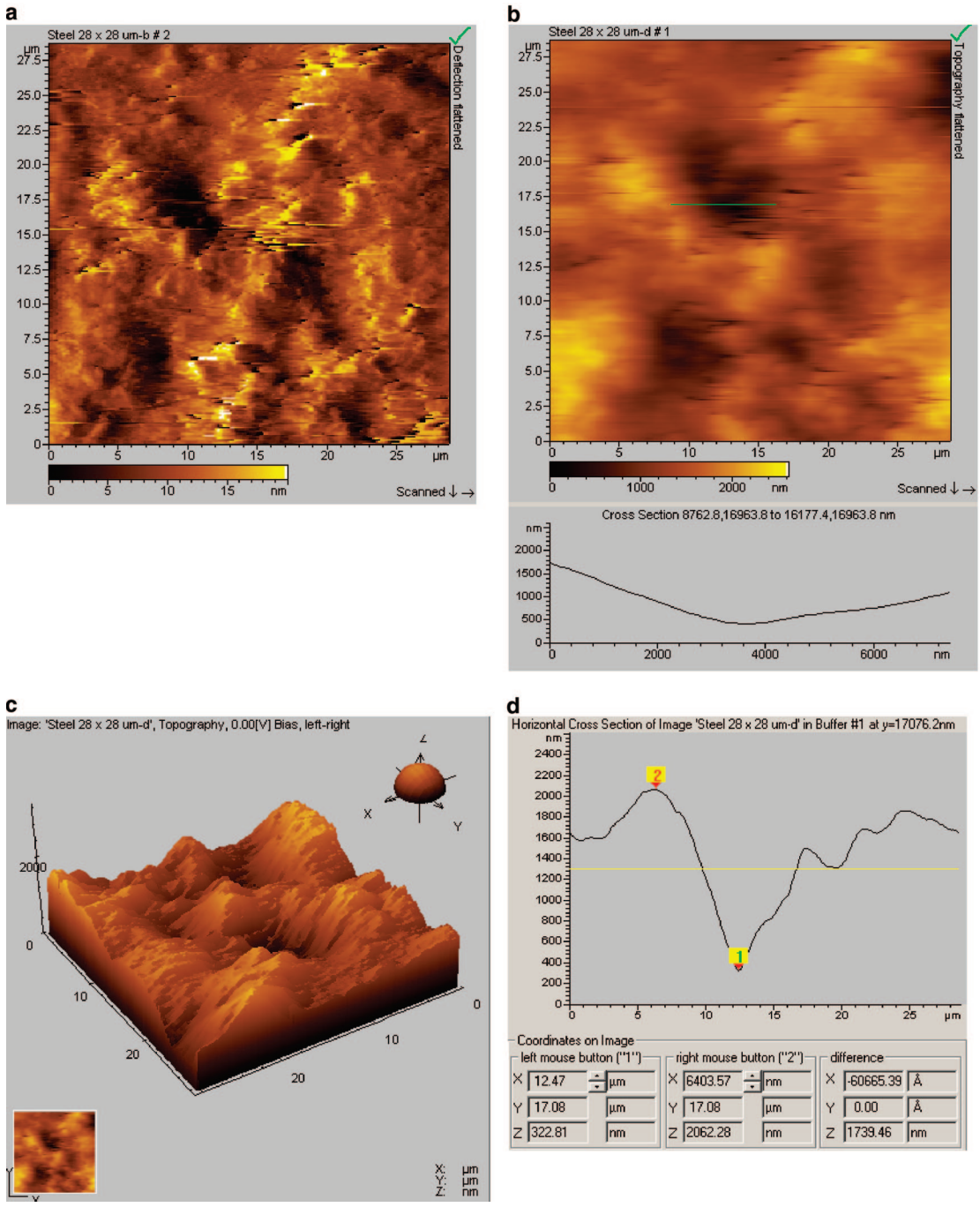

Figure 6. AFM images of corroded API 5L-X60 carbon steel surface exposed to ACE2 with the inhibitor system. (a) Two-dimensional topographic images of the corroded coupon surface (28 × 28 um). (b) Cross-sectional analysis determining the diameter of pit on the surface (0.7 μm). (c) Three-dimensional topographic images of the corroded coupon surface steel (pit size height). (d) Cross-sectional analysis determining the depth of pit on the surface (pit size, 1.6 μm).

The new peaks (system 4) at 1464 and 1378 cm^{-1} were noted due to CH chemical shift for the CH_3 group. The peak at 1021 cm^{-1} indicates the presence of the stable −C−O−C− group. The peak at 534 cm^{-1} indicates the presence of iron peak.[42] Though complex was formed on the metal surface, the degradation of inhibitor/diesel at the interface which act as humic substance (organic substance) results in a high supply of electrons to the metal surface and accelerates the corrosion.[43] It can be inferred that the corrosion inhibitor coordinated with Fe^{2+} through the −C−O−C− and carbonyl oxygen, resulting in the formation of Fe^{2+} corrosion inhibitor complex on the metal surface. In the present study, a water-soluble component (pyridine) dissolves in water and inhibits corrosion in the absence of bacterium ACE2. At the same time, ACE2 prefers the interface between organic and inorganic for utilizing energy from the organic phase where the oil-soluble inhibitor components (oleic acid, aminophenol, hexadecaneic acid) were consumed as the energy source rather than pyridine-based components. The biodegradation efficiency of this bacterium ACE2 and the corrosion rate of API 5L-X60 in the different systems in presence of ACE2 have been described in earlier studies.[21]

The extent of corrosion damage caused by the ACE2 in the presence/absence of inhibitor was assessed by profiling the pits on the coupon surface after the removal of biofilm. Representative pits were captured using AFM by randomly selecting four different areas on each coupon after exposure to the ACE2

inoculated system. Figure 5a,b and Figure 6a−d show the two- and three-dimensional topographic images of the corroded coupon surfaces (28 × 28 um) collected from systems 3 (inhibitor) and 4 (inhibitor with strain ACE2) after 10 days immersion. Figure 5a,b shows the surface topography of the inhibitor-added metal surface, where no significant pits on the surface (Figure 5c) were observed when compared to system 4 (Figure 6c). This reveals that the inhibitor forms a thin film on the metal surface and inhibits the corrosion. Figure 6b,d shows the cross-sectional analysis of pit surfaces, where the diameter and depth of the pit were 0.7 ± 0.12 μm and 1.6 ± 0.14 μm, respectively. This indicates that ACE2 accelerates the pitting corrosion on API 5L-X60 and also reduces the corrosion inhibition efficiency of the inhibitor. *S. marcescens* ACE2 is a facultative anaerobe, and biochemical tests indicate the presence of catalase and cytochrome oxidase. ACE2 has a peroxidase enzyme, which produces hydrogen peroxide for the degradation of corrosion inhibitor/diesel products. Moreover, it produces catalase that overcomes the toxic nature of hydrogen peroxide, breaking it down into water and oxygen.[44–46] During the respiratory process, oxygen is consumed by ACE2 and converted into water, wherein H^+ is utilized from the degraded inhibitor product and electrons are supplied by cytochrome oxidase enzyme.

It can also be assumed that ACE2 favors the Fenton reaction[41] (eqs 1 and 2) by reducing ferric iron, leading to the production of hydroxyl radicals that can damage any biological macromolecules.

$$1/2O_2 + 2H^+ + 2e \rightarrow H_2O \quad (1)$$

$$Fe^{2+} + H_2O_2 \rightarrow Fe^{3+} + OH^{\bullet} + OH^- \quad (2)$$

It is inferred that the formation of Fe^{3+} combines with OH^- ions and degraded products to form an iron−organic complex as corrosion product (Figure 4D). Hydrogen and carbon are consumed by ACE2 from hydrocarbon present in the inhibitor. The oxygen from peroxide and H^+ molecules from the degraded products combine with Fe^{2+} to produce Fe^{3+}. Since this bacterium lives in low-pH environments,[42] Fe^{3+} formation is encouraged by peroxide production and corrosion according to eq 2.

ACE2 further converts ferric ion to ferric oxides by inclusion of oxygen from the degraded products (eq 3), and finally the ferric organic complex may be formed as a corrosion product on the metal surface, as observed in the FTIR analysis (system 4).

$$Fe^{2+} + 1/4O_2 + H^- \rightarrow Fe^{3+} + H_2O_2 \quad (3)$$

Moreover, AFM studies have been carried out to examine the surface morphology of the coupons (Figure 5a,b). Pitting corrosion was detected in system 4. In the absence of the bacterium and in the presence of the corrosion inhibitor, a corrosion inhibition efficiency of about 48% was noted.[21] In the presence of inhibitor and the bacterium ACE2, the inhibition efficiency was reduced; the corrosion rate was effectively double that of the control. The results indicate that bacterium ACE2 degrades the inhibitor, which is consistent with our earlier observation[21] and reduces the efficiency of the inhibitor.[17] Hence, this bacterium reduces both anodic and cathodic inhibitor components by a degradation process that reduces the inhibition efficiency.

4. Conclusions

The performance of an organic film forming corrosion inhibitor was assessed for its corrosion inhibition efficiency for API 5L-X60 steel in a petroleum product containing bacterial contaminant ACE2. The bacterial attachment is heterogeneous in nature, which enhances the pitting corrosion of metal surface API 5L-X60 (system 2). In the presence of the bacterium, the inhibitor enhances the anodic reaction and suppressed the cathodic reaction significantly more than in the presence of inhibitor system 3. The electrochemical behavior of API 5L-X60 was correlated with the role of adsorbed amine-based compound and degraded product on the metal surface. A severe pitting type of corrosion was observed in system 4 (inhibitor with strain ACE2) when compared to system 3 (inhibitor). The reduction of anodic current in system 2 may be due to the biosurfactant production by ACE2 and form an intact surface film on the metal surface in low chloride environment. The surface film formed by the inhibitor along with strain ACE2 on metal surface was characterized. The many functional groups of inhibitor peaks including the −NH− stretch (water-soluble components) completely disappeared due to the utilization of a sole carbon source for bacterial growth. This shows that the strain ACE2 was able to accelerate the pitting corrosion by the utilization of inhibitor as a sole carbon source. The present study reveals that nonbiodegradable anodic and cathodic components of the inhibitor are needed in petroleum product pipelines in order to avoid the microbial degradation of corrosion inhibitors for higher corrosion inhibition efficiency.

Acknowledgment

The authors are grateful to the reviewers for valuable suggestions and critical evaluation of the manuscript.

Literature Cited

(1) Angostini, R. A.; Young, R. D. A case history: investigation of microbially influenced corrosion in a wet Texas waterflood. In *Proceedings of the NACE annual conference, corrosion/90*; NACE International: Houston, 1990; Paper 119, pp 1−14.

(2) Buck, E.; Maddux, G. C.; Sullivan, R. L. *Internal Corrosion Cost Impact Study—United States natural gas exploration and production industry*; GRI-96/0056 document No. 96-1466; Gas Research Institute: Des Plaines, IL, 1996.

(3) Farthing, S. Company combats MIC with aggressive control program. *Pipe Line Gas Ind.* **1997**, *80* (10), 43–47.

(4) Pope, D. H.; Pope, R. M. *Guide for the monitoring and treatment of microbiologically induced corrosion in the natural gas industry*; GRI report GRI-96/0488; Gas Research Institute: Des Plaines, IL, 1998.

(5) Kochzp, G. H.; Brongers, M. P. H.; Thompson, N. G.; Virmani, Y. P.; Payer, J. H. Corrosion costs and preservative strategies in the United States, FHWA-RD-01-156 (on-line); Federal Highway Administration: Washington, DC, 2001; http://www.corrosioncost.com.

(6) Little, B.; Ray, R. A perspective on corrosion inhibition by biofilms. *Corrosion* **2002**, *58*, 424–428.

(7) Beech, I. B.; Sunner, J. Biocorrosion, towards understanding interactions between biofilms and metals. *Curr. Opin. Biotechnol.* **2004**, *15*, 181–186.

(8) Bento, F. M.; Gaylarde, C. C. The production of interfacial emulsions by bacterial isolates from diesel fuels. *Int. Biodeterior. Biodegrad.* **1996**, *38*, 31–33.

(9) Muthukumar, N.; Mohanan, S.; Maruthamuthu, S.; Subramanian, P.; Palaniswamy, N.; Raghavan, M. Role of *Brucella* sp. and *Gallionella* sp. in oil degradation and corrosion. *Electrochem. Commun.* **2003**, *5*, 421–426.

(10) Rajasekar, A.; Ganesh Babu, T.; Karutha Pandian, S.; Maruthamuthu, S.; Palaniswamy, N.; Rajendran, A. Biodegradation and corrosion behaviour of *Bacillus cereus* ACE4 in diesel transporting pipeline. *Corros. Sci.* **2007**, *49*, 2694–2710.

(11) Papavinasam, S.; Review, W. R.; Panneerselvam, T.; Bartos, M. Standards for laboratory evaluation of oilfield corrosion inhibitors. *Mater. Perform.* **2007**, *46*, 46–51.

(12) Swidzinski, M.; Watson, J.; Mackin, K.; Jepson, W. P. Selection and optimization of *corrosion* inhibitor treatment for a new multi-phase pipeline operating under potentially corrosive conditions. *Corrosion* **2003**, *23*, 16–20.

(13) Jayaraman, A.; Saxena, R. C. Corrosion and its control in petroleum refineries—a review. *Corros. Prev. Control* **1995**, *42*, 123–131.

(14) Muthukumar, N.; Rajasekar, A.; Ponmariappan, S.; Mohanan, S.; Maruthamuthu, S.; Muralidharan, S.; Subramanian, P.; Palaniswamy, N.; Raghavan, M. Microbiologically influenced corrosion in petroleum product pipelines—a review. *Indian J. Exp. Biol.* **2003**, *41*, 1012–1022.

(15) Videla, H. A.; Gomez de Saravia, S. G.; Guiamet, P. S. Microbial degradation of film-forming inhibitors and its possible effects on corrosion inhibition performance. *Corrosion/2000*; NACE International: Houston, TX, 2000; paper no. 00386.

(16) Kirov, P. The influence of drag reducers and inhibitors on the rate and mechanism of corrosion in petroleum white products in the presence of moisture. *Electrochim. Acta* **1987**, *32* (6), 921–926.

(17) Freiter, E. R. Effect of a corrosion inhibitor on bacteria and microbiologically influenced corrosion. *Corrosion* **1992**, *48* (4), 266–276.

(18) Muthukumar, N.; Maruthamuthu, S.; Palaniswamy, N. Role of cationic and nonionic surfactants on biocidal efficiency in diesel-water interface. *Colloids Surf., B: Biointerfaces* **2007**, *57* (2), 152–160.

(19) Rajasekar, A.; Maruthamuthu, S.; Palaniswamy, N.; Rajendran, A. Role of corrosion inhibitor degradation and its influence on corrosion. *Microbiol. Res.* **2007**, *162*, 355–368.

(20) Rajasekar, A.; Maruthamuthu, S.; Muthukumar, N.; Mohanan, S.; Subramanian, P.; Palaniswamy, N. Bacterial degradation of naphtha and its influence on corrosion. *Corros. Sci.* **2005**, *47*, 257–271.

(21) Rajasekar, A.; Ganesh Babu, T.; Maruthamuthu, S.; Karutha Pandian, S.; Mohanan, S.; Palaniswamy, N. Biodegradation and corrosion behavior of Serratia marcescens ACE2 isolated from Indian-diesel transporting pipeline. *World J. Microbiol. Biotechnol.* **2007**, *23* (8), 1065–1074.

(22) Muthukumar, N.; Ilangovan, A.; Maruthamuthu, S.; Palaniswamy, N. Surface analysis of inhibitor films formed by 1-aminoanthraquinones on API 5L-X60 steel in diesel-water mixtures. *Electrochim. Acta* **2007**, *52*, 7183–7192.

(23) Xu, L. C.; Chan, K. Y.; Fang, H. H. P. Application of atomic force microscopy in the study of microbiologically influenced corrosion. *Mater. Charact.* **2002**, *48*, 195–203.

(24) Homel, R. K. Formation and physiological role of biosurfactants produced by hydrocarbon-utilizing microorganisms. *Biodeterioration* **1990**, *1*, 107–116.

(25) Jana, J.; Jain, A. K.; Sahota, S. K.; Dhawan, H. C. Failure analysis of oil pipelines. *Bull. Electrochem.* **1999**, *15*, 262–265.

(26) Rahman, K. S. M.; Thahira, J.; Rahman, Y.; Kourkoutas, I.; Petsas, R.; Marchant Banat, I. M. Enhanced bioremediation of n-alkane in petroleum sludge using bacterial consortium amended with rhamnolipid and micronutrients. *Bioresour. Technol.* **2003**, *90*, 159–168.

(27) Reisfeld, A.; Rosenberg, E.; Gutnick, D. Microbial degradation of crude oil: factors affecting the dispersion in sea water by mixed and pure cultures. *Appl. Microbiol.* **1972**, *24*, 363–368.

(28) Finnerty, W. R.; Singer, M. E. A microbial biosurfactant physiology, biochemistry, and applications. *Dev. Ind. Microbiol.* **1984**, *25*, 131–146.

(29) Lang, S.; Wagner, F. Structure and properties of biosurfactant. In *Biosurfactants and Biotechnology Surfactant Science Series*; Kosaric, N., Cairns, W. L., Gray, N. C. C., Eds.; Marcel Dekker: New York, 1987; p 2145.

(30) Koch, K. A.; Kappeli, O.; Fiechter, A.; Reiser, J. Hydrocarbon assimilation and biosurfactant production in Pseudomonas aeruginosa mutants. *J. Bacteriol.* **1991**, *173*, 4212–4219.

(31) Maruthamuthu, S.; Mohanan, S.; Rajasekar, A.; Muthukumar, N.; Ponmarippan, S.; Subramanian, P.; Palaniswamy, N. Role of corrosion inhibitors on bacterial corrosion in petroleum product pipeline. *Indian J. Chem. Technol.* **2005**, *12*, 567–575.

(32) Ashassi Sorkhabi, H.; Nabavi-Amri. Polarization and impedance methods in corrosion inhibition study of carbon steel by amines in petroleum-water mixtures. *Electrochim. Acta* **2002**, *47*, 2239–2244.

(33) Denyer, S. P. Mechanism of action of biocides. *Int. Biodeterior. Biodegrad.* **1990**, *26*, 89–100.

(34) Lu, R. C.; Cao, A. N.; Lai, L. H.; Xiao, J. X. Interaction between lysozyme and mixtures of cationic-anionic surfactants decyltriethylammonium bromide-sodium decylsulfonate. *Colloids Surf., B: Biointerfaces* **2007**, *54*, 20–24.

(35) Syugaev, A. V.; Lomaeva, S. F.; Reshetnikov, S. M. Corrosion of Iron and Iron-Silicon Finely Dispersed Systems in Neutral Media. Part III. Fe-Si Systems Prepared by Milling in Pure Heptane or with Oleic-Acid. *Prot. Met.* **2006**, *42*, 315–322.

(36) Sastri, V. S. *Corrosion Inhibitors: Principles and Applications*; Wiley: New York, 1998.

(37) Sheng, X.; Ting, Y. P.; Pehkonen, S. O. Evaluation of an organic Corrosion Inhibitor on Abiotic Corrosion and Microbiologically Influenced Corrosion of Mild Steel. *Ind. Eng. Chem. Res.* **2007**, *46*, 7117–7125.

(38) Patel, N. K. Corrosion Inhibitors for 63/37 brass in trichloroacetic acid solution. *J. Electrochem. Soc.* **1972**, *21*, 136.

(39) Papavinasam, S.; Review, R. W.; Attard, M.; Demoz, A.; Sun, H.; Donini, J. C.; Michaelian, K. H. Laboratory methodologies for corrosion inhibitor selection. *Mater. Perform.* **2000**, *39*, 58–60.

(40) Tan, Y. S.; Srinivasan, M. P.; Pehkonen, S. O.; Chooi, S. Y. M. Effects of ring substituents on the protective properties of self-assembled benzenethiols on copper. *Corros. Sci.* **2006**, *48*, 840–862.

(41) Bentiss, F.; Traisnel, M.; Vezin, H.; Lagrenee, M. Electrochemical Study of Substituted Triazoles Adsorption on Mild Steel. *Ind. Eng. Chem. Res.* **2000**, *39* (10), 3732–3736.

(42) Jones, D. A.; Amy, P. S. Related Electrochemical Characteristics of Microbial Metabolism and Iron Corrosion. *Ind. Eng. Chem. Res.* **2000**, *39* (3), 575–582.

(43) Cervantes, F. J.; Dijksma, W.; Duong-Dac, T.; Ivanova, A.; Lettinga, G.; Field, J. A. Anaerobic Mineralization of Toluene by Enriched Sediments with Quinones and Humus as Terminal Electron Acceptors. *Appl. Environ. Microbiol.* **2001**, *67*, 4471–4478.

(44) Busalmen, J. P.; Vazquez, M.; de Sanchez, S. R. New evidence on the catalase mechanism of microbial corrosion. *Electrochim. Acta* **2002**, *47*, 1857–1865.

(45) Touati, D. Iron and oxidative stress in bacteria. *Arch. Biochem. Biophys.* **2000**, *373* (11), 1–6.

(46) Angerer, A.; Klupp, B.; Braun, V. Iron transport systems of *Serratia marcescens*. *J. Bacteriol.* **1992**, *174* (4), 1378–1387.

(47) Young, J. A. Chemical Laboratory Information Profile: Oleic Acid. *J. Chem. Educ.* **2002**, *79*, 24–30.

(48) Driesbach, R. R. *Physical Properties of Chemical Compounds*; American Chemical Society: Washington, DC, 1961; Vol. 3.

(49) Shimizu, S.; Watanabe, N.; Kataoka, T.; Shoji, T.; Abe, N.; Morishita, S.; Ichimura, H. Pyridine and Pyridine Derivatives. In *Ullmann's Encyclopedia of Industrial Chemistry*; John Wiley & Sons: New York, 2007.

(50) Pool, W. O.; Ralston, A. W. Boiling Points of n-Alkyl Acids. *Ind. Eng. Chem.* **1942**, *34*, 1104.

Received for review April 13, 2008
Revised manuscript received June 11, 2008
Accepted June 20, 2008

IE8005935